Effect of Substrate Temperature on the Structural and Optical Properties of CuO-CaO2 Composite Thin Film Prepared by PSP

Sayad Mostefa^{1,2}, Ouahab Abdelouahab¹, Belakroum Karima², Rahmane Saâd¹, Kater Aicha¹, Hettal Souheila¹, Ben Messaoud Ouarda¹

¹Laboratory of Thin Films Physics and Applications (LTFPA), Mohamed Khaider Biskra University, BP 145 RP, 07000 Biskra, Algeria.

²Laboratory for the Development of New and Renewable Energy in Arid and Saharan Areas (L.D.N.R.E.A.S.A), Kasdi Merbah Ouargla University, BP 511, 30 000 Ouargla, Algeria. Email: s.mostefa1991@gmail.com

This studying hand deals with the investigation of the deposition of a combination of copper oxide and calcium oxide thin films through pneumatic spray pyrolysis (PSP) at varying substrate temperatures (450, 500, 550, and 600±5 °C). Two sources of copper chloride and calcium chloride, both with equal molarity dissolved in distilled water were utilized. The impact of substrate temperature on the films structural, morphological, optical, electrical, and dielectric properties was assessed using several analytical techniques, including X-ray diffraction, scanning electron microscopy, and energy dispersive spectroscopy. The X-ray diffraction results revealed the simultaneous growth of CuO and CaO2 on the substrate. The band gaps of the films were determined through UV-visible transmission and reflection measurements. The results showed that all films were polycrystalline, with increasing substrate temperature leading to an increase in film thickness from 641,79 to 735,87 nm and an average calculated grain size between 33.71 and 63.73 nm. The optical band gaps were found to range between 1.63 and 2.80 eV. The dielectric constant is obtained for the film deposited at 600 °C with a value of about 6.5.

Keywords: thin film, spray pyrolysis, copper oxide, calcium oxide, optoelectronic properties, dielectric properties.

1. Introduction

In the world of electronics, optoelectronic and electronic devices have enjoyed rapid development in recent years and these devices have contributed to the employment of many applications. Metal oxide materials are considered an important part in the development of these devices, especially semiconductors made of metal oxide. Copper oxide was a prevalent oxide for research in the past and is still the subject of ongoing studies, either in its pure form or when mixed with other oxides. Recent studies have focused on the properties of copper oxide when mixed or doped with elements like Zn, Mg, Al, and Ca etc... [1-4]. Most studies have focused on the growth and optical properties of copper oxide [5], considered as nontoxic, economically viable, and environmentally friendly. It is also attractive due to its easy formation [6]. Cupric oxide (CuO) and cuprous oxide (Cu2O) are the two common forms of copper oxide, both of which are p-type semiconductors and have monoclinic and cubic structures with band gap values of 1.3–2.1 eV and 2.0–2.6 eV, respectively [7], and are able to have n-type conductivity with doping by donor material [8]. These phases have suitable properties for specific applications such as electrode materials for lithium batteries [9], gas sensors [10], and pn junction diodes [11]. researchers in the last few years discovered that bulk CuO exhibits the multiferroic phase in a narrow temperature range (213 K to 230 K) and can it used in a variety of applications [12], Thanks to many techniques that led to reducing the size of materials to the nanoscale, which resulted in the development of new and unique behaviors for many materials in structural, optical, electrical, and dielectric properties [13]. Copper oxide CuO exhibits a high value of dielectric constant of about 18.1[14]. Various techniques have been used to prepare copper oxide films, including sol-gel [15], chemical vapor deposition [16], electro-deposition [17], plasma evaporation [18], thermal evaporation [19], reactive magnetron sputtering [20], pneumatic spray pyrolysis technique [21,22]. Calcium oxide (CaO), in turn, finds use in a wide range of applications in materials research. Pure CaO has a rock salt structure with a lattice parameter a = 0.481059nm [23,24] and may be found as a transparent crystalline solid or white amorphous material [23]. It has a wide band gap of 7.085 eV [25], making it an attractive material for applications where electrical isolation is required. Thin film technology has contributed to expanding the fields of applications such as transparent electronic applications [26], solar cells [27], and CaO is used for its ability to modify electrical and dielectric properties, with a high dielectric constant of 11.8 [28]. The dielectric function consists of a part of free electron contribution and a part of interband transition [29]. CaO is used as a dopant or component of composite material, it was reported as a dopant is able to stabilize cubic zirconia [30,31], and was found as a compound in calcium alumina oxide phases CaO.Al₂O₃ [32], calcium manganese oxide Ca₃Mn₂O₇ [33], Calcium fluoride CaF₂ thin films [34], biodiesel production catalyzed by CaO nanocatalyst [35]. A. Bouibes was investigated CaO₂ as new thermodynamically stable compound [36]. Some reports on the fabrication of CaO films including Pulsed Injection Metal Organic Chemical Vapour Deposition (PI-MOCVD) [23], ultrasonic-assisted synthesis of Ca(OH)2 and CaO [28], fabrication of CaO insulator coatings by MOCVD for application in vanadium/lithium blankets [37], chemical bath deposition (CBD) method [38], Thermal-decomposition [39], sol-gel [40], Direct Precipitation Technique (DPT) [41].

As mentioned above, both copper oxide and calcium oxide have many applications, whether

as pure oxide or as a component with another substance, there are many applications and optoelectronic devices where buffer layers are used as a barrier to prevent interference between conductive parts or for other purposes such as solar cells, light-emitting diodes, and transistors. Appropriate materials must be carefully selected to obtain an insulating layer and the required conditions must be provided. Z. Yu et al. were able to deposit a thin layer of copper-calcium (CuCa) as a buffer layer under optimal conditions and tested it as a diffusion barrier to prevent the diffusion of copper atoms in silicon-based materials (substrate) during deposition [42].

This study aimed mainly to search for the phase of Ca and Cu oxides complex and observe the effect of substrate temperature on the films structural, morphological, optical, electrical, and dielectric properties by utilizing two sources of copper chloride and calcium chloride with equal molarity to deposit a combination of copper oxide and calcium oxide thin films. We have chosen the pneumatic spray pyrolysis technique because it is homemade and in contrast to other methods has distinct advantages such as simplicity, cost-effectiveness, ecofriendliness, economical, operating at room temperatures, and potential controllability, which plays a vital role in the ease of producing a large number of samples.

2. Experimental details

In this study, thin films were generated by mixing two sources, copper chloride ($CuCl_2-2H_2O$) and calcium chloride ($CaCl_2-2H_2O$), in a solution with a concentration of 0.1 M for each source (0.1:0.1 M). The solution was prepared by dissolving the sources in 50 ml of distilled water at room temperature. The films were deposited on glass substrates using a homemade pneumatic spray pyrolysis technique at different substrate temperatures of 450, 500, 550, and 600 ± 5 °C. The deposition process involved spraying the solution onto the heated substrates using compressed air and a nozzle atomizer. The deposition time was fixed to 3 minutes, and the distance between the spray nozzle and the substrate was kept constant at 30 cm. The resulting samples were labeled S_1 , S_2 , S_3 , and S_4 , with each label corresponding to the substrate temperature used during deposition. The samples were allowed to cool gradually to room temperature after the deposition process was completed. Various characterization techniques were employed to investigate the properties of the thin films. The obtained results are presented in the following section.

3. Results and discussions

The thicknesses of thin films were measured using the approximate gravimetric method which consists of weighting the substrate before and after deposition (Δm) with an accurate balance. The density (g) of the material of the films and the surface substrate (A) give access to the thickness using the following equation [43,44]:

$$d = m/(g * A) \tag{1}$$

It was found that the thickness of the films approximately increases when the substrate temperature is increased as shown in Table 1. The growth velocity (G_v) of the films is then calculated by the following formula [45]:

Nanotechnology Perceptions Vol. 20 No.6 (2024)

$$G_{v} = d/t \tag{2}$$

Where d is the thickness of the film and t is the time of deposition.

Table 1 shows the variation in the thickness and growth rate with respect to the substrate temperature, in addition to measurement errors, which often exist because the measurement is manual and difficult to control compared to measuring devices that are accurate, and since there are errors in measuring thickness, it is known that there are measurement errors as well in all characteristics in which the thickness is used for calculation. From the Table 1, it appears that the thickness of the thin films increases with increasing substrate temperature except for 550 °C where a decrease in film thickness appears. This decrease in thickness can be explained by the fact that the substrate temperature is sufficient for a good reaction of the sprayed droplets and thus provides optimum rate of thermal energy to give good film quality. Perhaps this will be confirmed after analyzing the properties of thin films. Also it is noticed that the growth rate increases slightly with increasing substrate temperature except for 550 °C. This is related to the increase in film thickness which can be explained by the increase in the amount of atomized droplets that carry the particles (arriving species flow) hence rising the rate of their accumulation on the heated substrate. It is well known that the increase in thermal energy leads to rapid chemical reactions and thus allows more growth of nucleated particles on the substrate surface by giving more energy to allow migration of species and coalescence of the particles on the substrate.

Table 1: Thickness and growth rate of our thin film samples.

		8	I	
Sample	Temperature	Thickness	Growth rate	
	(°C)	(nm)	(nm/min)	
S_1	450	$641,79 \pm 144,65$	213,93	
S_2	500	$721,80 \pm 156,70$	240,6	
S_3	550	$694,12 \pm 149,65$	231,37	
S_4	600	$735,87 \pm 140,33$	245,29	

3.1. Structural properties

The structure of the thin film samples was studied by X-ray diffraction analysis (XRD) using Rigaku-Type MiniFlex 600 with Cu K α radiation ($\lambda = 1.5418$ Å). The results are shown in fig. 1. The XRD results analysis indicates clearly that the film structure changes when the substrate temperature increases. We notice, as shown in fig. 1, that all films are polycrystalline because of the presence of various diffraction peaks (JCPDS N° 03-065-2309 for CuO, and JCPDS file N°00-003-0865 for CaO₂).

We can see also that some of the diffraction peaks disappear and some other diffraction peaks appear when the substrate temperature increases. The diffraction peaks at 2θ = 35°, 38°, and 53° are present for all the films. Meantime it is observed that the number of diffraction peaks decreases with increasing substrate temperature indicating the change in the film's crystalline structure. A close insight into the XRD diffractograms shows that there are some diffraction peaks containing two or three joint peaks resulting from diffraction planes of different phases (see Fig. 2). In fact, the films contain calcium oxide CaO₂, copper oxide CuO, and Cu₂Cl₂O as shown in Fig. 1 and confirmed by the electron energy dispersive spectroscopy (EDS) analysis. We notice that for the films produced at the substrate temperature of 450 and 500 °C, the phase Cu₂Cl₂O appears(2θ = 31.76°) which has other diffraction peaks merged in some other peaks but with very low relative intensity as shown

in the XRD diffractograms. Since it disappears at higher substrate temperatures (550 and 600 °C); it is very likely that this phase does not have enough time to evaporate. Also, when we observe the films produced at the substrate temperature of 550 and 600 °C, we find that the same diffraction peaks appear in these two samples which indicates that substrate temperature at 550 °C is the optimum rate of thermal energy to crystallize the film. The results also showed no Ca-Cu-O compound (mixed phase) between the two oxides.

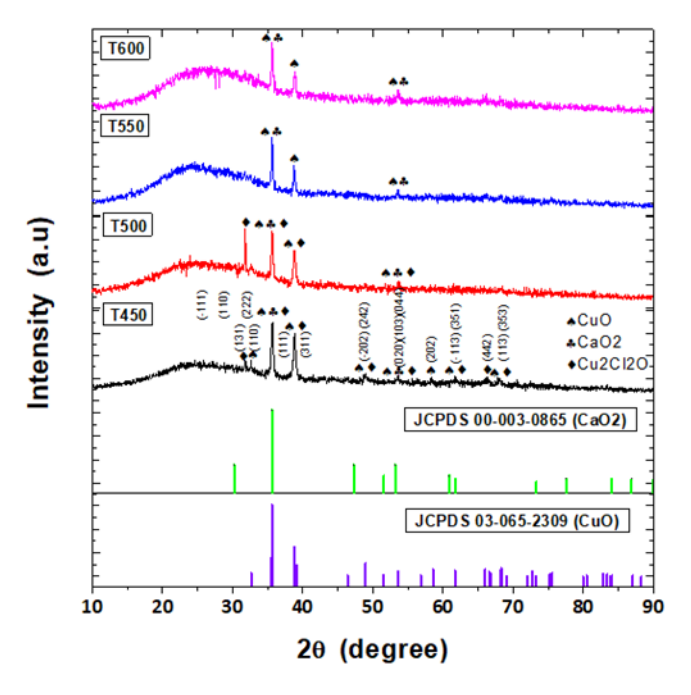


Fig. 1. X-ray diffraction patterns of the studied samples.

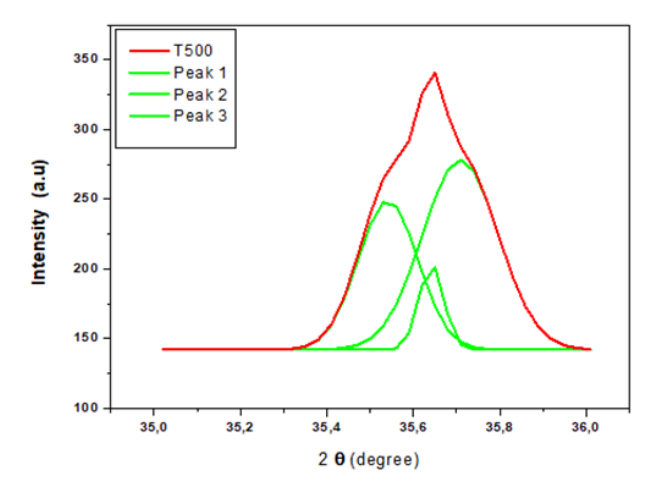


Fig. 2. X-ray diffraction pattern of the peak of sample S_2 at $2\theta = 35^\circ$.

The grain size (D), the dislocation density (δ), and the microstrain (ϵ) give information about

important structural properties. The grain size is obtained from the Scherrer formula [46]:

$$D = k \lambda / \beta \cos \theta \tag{3}$$

Dislocation density (δ) and microstrain (ϵ) are estimated by:

$$\delta = 1/D^2 \tag{4}$$

$$\varepsilon = \beta \cos \theta / 4 \tag{5}$$

Where k is the shape factor (0.94), β is the full-width at half-maximum FWHM, θ is the Bragg angle, and λ is the wavelength of theused X-rays. The calculated average of grain size (D), dislocation density (δ), and microstrain (ϵ) of our samples at the two diffraction peaks $2\theta = 35^{\circ}$, 38° are given in Table 2.

It is seen in Table 2 that the average grain size increases with increasing substrate temperature from 450 up to a maximum of 550 °C, from 33.71 nm to 63.73 nm and then decreases to 45.47 nm at 600 °C. The decrease in grain size indicates a phase change and recrystallization process in the polycrystalline thin films. When depositing the film, many common stresses can occur, including: thermal stress resulting from the difference of expansion coefficient of the film and substrate and internal stress due to the accumulating effect of the crystallographic flaws built into the film during deposition [47]. Also a strain maybe created between crystalline lattices of two oxides. The microstrain and dislocation density show the opposite behavior, where, the values of δ and ϵ decreases with increasing substrate temperature from 450 to 550 °C and then increases at 600 °C. The decrease in microstrain and dislocation density to substrate temperature 550 °C denotes that the film is improving up to this temperature. It is known that the increase in grain size leads to a decrease in the grain boundaries and hence minimizing the number of defects in the structure. Besides, this mechanism enhances the films stabilization. The decrease in microstrain and dislocation density denotes that the lattice defects along grain boundaries become less important and vice versa [48].

Table 2: The average grain size (D), dislocation density (δ) and microstrain (ϵ) of thes amples at the two diffraction peaks $2\theta = 35^{\circ}$, 38° .

Sample	2θ (°)	Average D (nm)	Dislocation density $\delta \times 10^{14}$ (lines/m ²)	Microstrain ε ×10 ⁻⁴
S_1	35.6764 38.8474	33.7157	8.7970	11.4746
S_2	35.6350 38.8344	61.1324	2.6758	5.9223
S_3	35.6180 38.7766	63.7314	2.4620	5.9285
S_4	35.6294 38.8566	45.4768	4.8352	8.9871

3.2. Morphological and elemental analysis

The surface morphology of our samples deposited at different substrate temperature is investigated by scanning electron microscopy (SEM) using TESCAN VEGA3 SEM as shown in Fig. 3. The optical and electrical properties of the films are affected by the properties of the surface [49]. It is clearly observed that the increase in the temperature of the substrate improves the surface morphology. With the same magnification, the film surface

shows a change in the morphology of the samples when the substrate temperature changes. It is also observed that the samples do not show any cracks and their surfaces are dense and compact (no porous or hollow regions are observed) for all substrate temperatures. Samples S_1 (a) and S_2 (b) have uniform distribution and homogeneous particles on the surface, whereas sample S_2 (b) shows the beginning of the appearance of very fine particles. Samples S_3 (c) and S_4 (d) show different agglomerations at different locations of the particles on the surface. This is thought to be caused by the speed of deposition of particles where some of which evaporate before reaching the substrate owing to the increase in the substrate temperature. The increase in film thickness also affects the surface distribution.

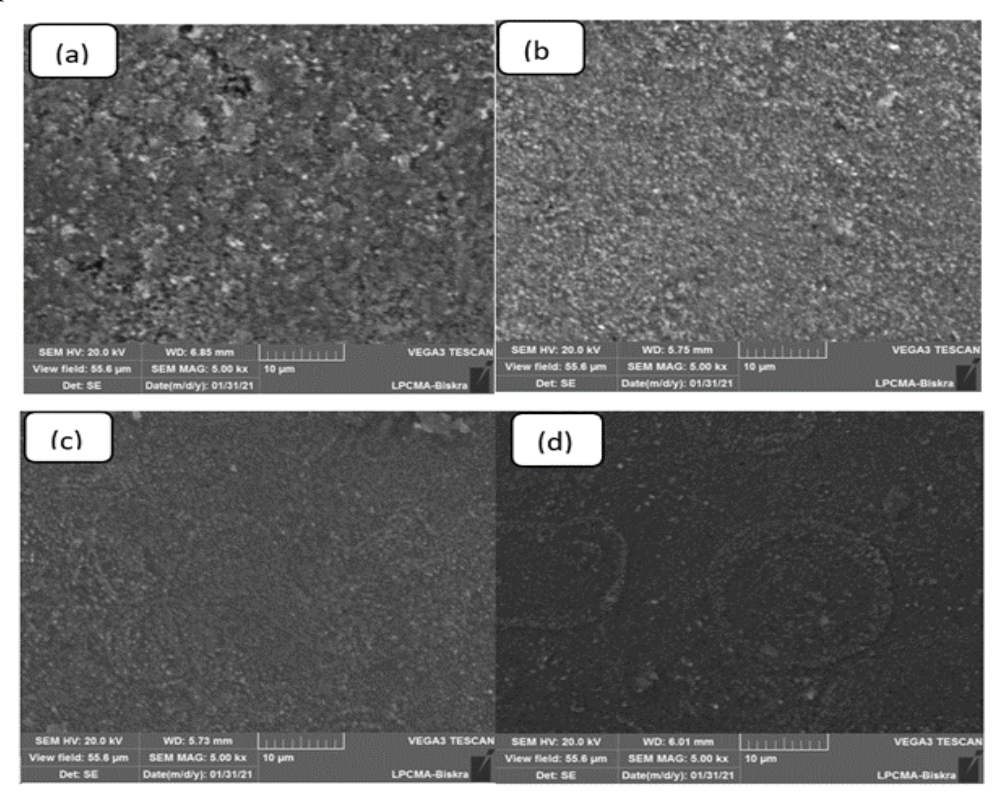


Fig. 3. Surface Morphologies of the samples deposited at various substrate temperatures (a) 450 °C, (b) 500°C, (c)550 °C, and(c) 600 °C.

The EDS analysis is used to confirm the composition of the films. The results of the EDS analysis are shown in fig. 4. These spectra confirm the presence of Cu, Ca, and O elements in the films, In addition to the atomic composition ratio of all particles in all samples prepared at different substrate temperatures.

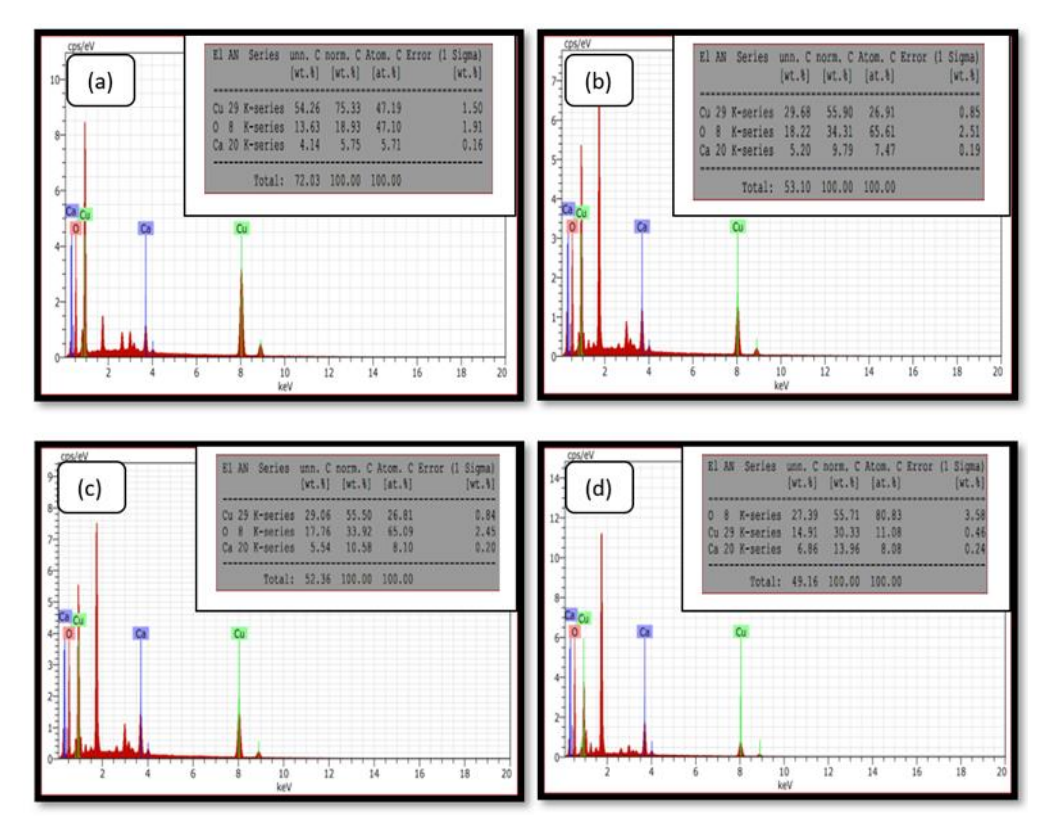


Fig. 4. EDS spectra of the samples deposited at various substrate temperatures (a) 450 °C, (b) 500°C, (c) 550 °C, and (d) 600 °C.

3.3. Optical properties

The optical transmittance and reflection spectra of the thin films were investigated by a UV-Visible spectrophotometer at room temperature using a JACSO V-770 spectrophotometer. Fig. 5 shows the optical transmittance curves as a function of wavelength in the range of 300 to 1200 nm. It is clear that the optical transmittance increases with increasing substrate temperature. The spectra show that the transmittance values of the films increase sharply near 800 nm which represents the absorption edge in the visible region. Also the films behave as transparent in near-infrared region (NIR), this indicates a good films quality. Whereas, the films behave as dense and opaque material in the region below 700 nm because of the low transmittance values in this range due to the strong absorption by electrons moving from the valence band to the conduction band (transitions) at the beginning of the incident light (low wavelengths). The increase in transmission with increasing substrate temperature indicates a decrease in electronic transitions from the valence band to the conduction band, which are known to be responsible for the absorption of light photons, although the thickness increases. A lower transmission is observed at lower temperatures of 450 °C which the sample appears in black color, and this may be due to an incomplete reaction between the composites of the sprayed droplets. As can be seen in Fig. 5, the optical transmission of the sample S₃ (550 °C) is the highest (65%) which the sample appears in a light black color.

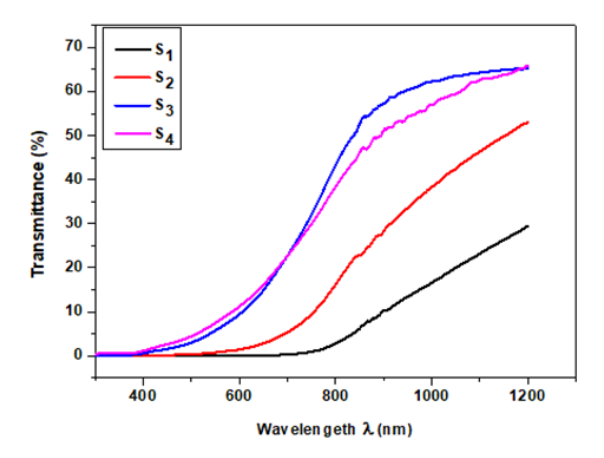


Fig. 5. Transmission spectra of our samples deposited with different substrate temperatures.

The reflection spectra of the samples are shown in fig. 6. It can be clearly seen that when the temperature of the substrate increases, the reflection increases. The reflection values are low and remain almost constant below 700 nm. Also, the values of the reflection for S_1 and S_2 films are very low compared to S_3 and S_4 in this region. The average reflectance is less than 20%. The transmittance and reflectance spectra (Fig. 5 and 6 respectively) show that the films exhibit low absorbance with both changes in substrate temperature and wavelengths in this region, at 800 nm, there is a significant increase in the film's reflection, especially for S_1 and S_2 . It is noticeable that in this range the transmittance also rises with rising substrate temperature, which indicates that the film absorption of light in this wavelength domain diminishes when substrate temperature rises. For wavelengths higher than 800 nm, we notice that the reflection of samples S_1 and S_2 decreases while for samples S_3 and S_4 continues to increase and thus the absorption of NIR photons rises for S_1 and S_2 and decreases for S_3 and S_4 .

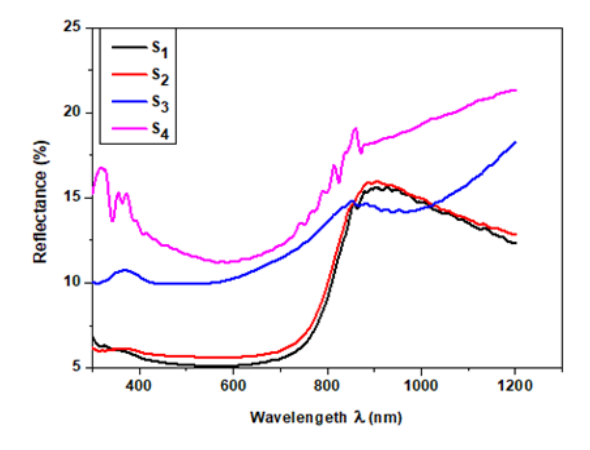


Fig. 6. Reflectance spectra of samples deposited at different substrate temperatures.

The optical band gap (Eg) is one of the important optical and electronic properties of *Nanotechnology Perceptions* Vol. 20 No.6 (2024)

semiconductors and insulators. The optical method is used to determine Eg from the transmittance and reflectance measurements via the following formula [50,51]:

$$\alpha h \nu = A(h \nu - E_g)^n \tag{6}$$

Where hv is the energy of the photons, A is an independent constant of the energy, n is a coefficient depending on the type of transition (electronic transitions), n = 1/2 and n = 2 for direct and indirect transition, respectively [52]. α is the absorption coefficient calculated using the following formula [53,54]

$$\alpha = (1/d)\ln(1/T) \tag{7}$$

Where d is the sample thickness, and T is the transmittance. Fig. 7 shows the absorption coefficients recorded for the samples as a function of the wavelength. In general, as the incident light wavelength increases, the absorption coefficients are found to decrease for the same sample. It is also remarked that it decreases with the increase in substrate temperature, as mentioned above, at the beginning of the incident light, the absorption is strong due to the large number of electron transitions and then it demises to zero at high wavelengths because the films become transparent in this region. This is expected because of both the transmittance and reflection increase. As the substrate temperature increases, the absorbance and absorption coefficient decrease.

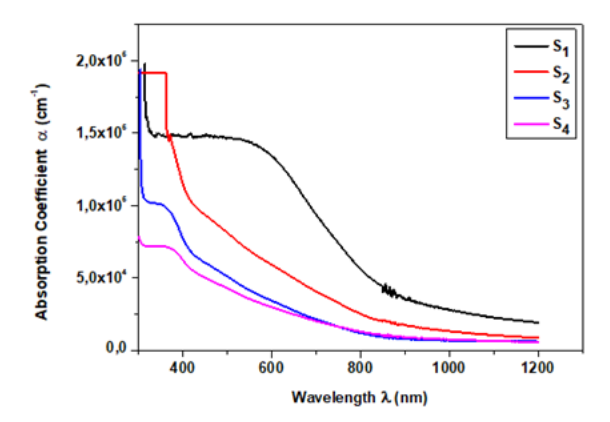


Fig. 7. Variation of the absorption coefficient of the samples as a function of the wavelength at different substrate temperatures.

The extrapolation of the linear part of the curve $(\alpha hv)^2 = f$ (hv) to $(\alpha hv)^2 = 0$ gives the direct band gap energy [55]. The direct optical band gaps Eg for thin films deposited with different substrate temperatures are listed in Table 3. As seen from this Table, the optical band gap exhibits a sharp increase with increasing substrate temperature from 1.63 eV at 450 °C to a maximum value of 2.87 eV at 500 °C and then gradually decreases until 600 °C. This sharp increase in the optical band gap from 450 °C to 500 °C indicates that the temperature at 450 °C is not sufficient for an interaction to occur between the reactants, and this is shown by giving the highest value for the Urbach energy at this temperature. The gradually decreases in the optical band gap from 2.87 to 2.68 eV probably due to the creation of tail bands between the valence and conduction bands, which result from traps and disorder present between the grains and generate states in the crystal structure, thus narrowing the kinetic and active *Nanotechnology Perceptions* Vol. 20 No.6 (2024)

distance of the band gap [43].

Urbach's energy is known to be related to the slope of the tails of localized states near the band edge that extend into the gap. It is common that these band tail states are responsible for absorption in the low energy range. Hence, the absorption coefficient is given by the following formula [56]:

$$\alpha(h\nu) = \alpha_0 \exp(h\nu/E_{IJ}) \tag{8}$$

Where α_0 is the pre-exponential factor, hv the photon energy, and E_U the band tail width or energy of disorder commonly called an Urbach tail. E_U can be extracted from the inverse slope of the linear plot between $ln(\Box)$ versus (hv). The Urbach's energy values are listed in Table 3. The Urbach's energy decreases with increasing substrate temperature. It was interpreted that the decrease of E_U with temperature indicates the smaller density of localized states created. Also, this means that as the substrate temperature increases the degree of disorder in the band gap decreases. This is due probably to the amelioration of the crystalline quality of the samples with the increase in substrate temperature as seen in the XRD section. This effect is also remarked by Shadia et al. for CdS:In thin films [57]. The slight increase in Urbach's energy value of sample 4 at higher substrate temperature may result from a decrease in grain size due to the recrystallization process.

By comparing our samples deposited from a mixture of calcium and copper oxide with other mentioned works in which pure copper oxide was deposited with changing substrate temperatures, we notice that there is a different behavior for pure copper oxide compared to our samples in all its properties, as reported in the references [58-60], which indicates that copper oxide is affected when mixed with calcium oxide.

Other optical properties of the samples can be deduced from the optical measurements such as refractive index (n) and extinction coefficient (k). The optical parameters n, k of our samples can be calculated by the formula [61,62]:

$$n = (1 + R^{1/2}/1 - R^{1/2}) \tag{9}$$

$$k = \alpha \lambda / 4\pi \tag{10}$$

Where R is reflection, α is absorption coefficient λ is the wavelength and k is extinction coefficient.

Table 3: n, k, ϵ_r and ϵ_i (at $\lambda = 800$ nm taken as comparison wavelength), Eg, E_U for thin films at different substrate temperatures: 450, 500, 550, and 600 °C

Sample	n	k	$\epsilon_{ m r}$	$\epsilon_{ m i}$	$E_g(eV)$	$E_{U}(eV)$
S_1	1,8696	0,3589	3,3666	1,3422	1,63	0,98
S_2	1,9188	0,1616	3,6556	0,6201	2,87	0,76
S_3	2,1673	0,0775	4,6915	0,3360	2,80	0,70
S_4	2,3970	0,0837	5,7387	0,4014	2,68	0,85

The dielectric constant ε is defined as a fundamental optical parameter and it is composed of two parts. It is given as follows [63]:

$$\varepsilon = \varepsilon_{\rm r} + \varepsilon_{\rm i} \tag{11}$$

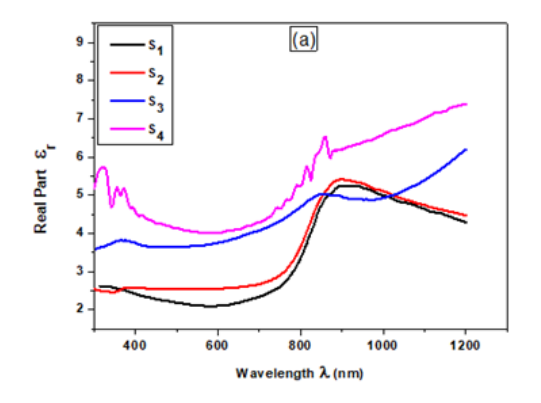
Where ε_r is the real part, allied to the stored energy within the material, and generally relates

to dispersion and ε_i is the imaginary part of the dielectric constant, related to the dissipation of energy inside the material [52]. The values of ε_r and ε_i are calculated using the following equations [64,65]:

$$\varepsilon_{\rm r} = {\rm n}^2 - {\rm k}^2 \tag{12}$$

$$\varepsilon_{i} = 2nk$$
 (13)

Fig. 8 shows the variation of the real and imaginary parts of the dielectric constant as a function of the wavelength. In Fig. 8a, the real part remains almost constant in the range of 300-700 nm for each sample but it increases with increasing substrate temperature. Near wavelength 800 nm the real part increases with increasing wavelength and substrate temperature in general but samples S₁ and S₂ exhibit an increase followed by a decrease. The increase in the real part near 800 nm for all samples is related to a sharp increase in transmittance in this region representing the absorption edge in the visible region. In Fig. 8b, the imaginary part of the dielectric function shows an increase and then a decrease with respect to the wavelength for all samples. The wavelength at which this happens decreases dramatically from 600 to 400 nm as the substrate temperature rises from 450 to 600 °C. The values of ε_r and ε_i obtained at $\lambda = 800$ nm, are listed in Table 3, together with n and k. The ε_r values are higher than that of ε_i values. Also, from Table 3 and Fig. 9a, it is clear that the real part increases with increasing substrate temperature while the imaginary part behaves otherwise. The real part of the dielectric constant increases from 3.36 to 5.73 with the increase of substrate temperature; endorsing the previous conclusions about the amelioration of the structure quality and the densification of the films. The highest value for the real part was obtained for the highest substrate temperature of 5,73 at 600 °C, which may be due to the high dispersion in the medium of material. It's known that the imaginary part of the dielectric constant is related to the extinction coefficient. The decrease of ε_i with the substrate temperature is due to the fact that in the samples at high substrate temperature, the films become decreasingly absorbers (Fig. 7), hence a low extinction coefficient, and consequently the imaginary part of the dielectric constant reached the lower values (Table 3). Fig. 9b shows the variation of extinction coefficient and refractive index with different substrate temperatures. From this figure, we notice that there is an inverse relation between n and k; that is, as the substrate temperature increases, n increases, and k decreases.



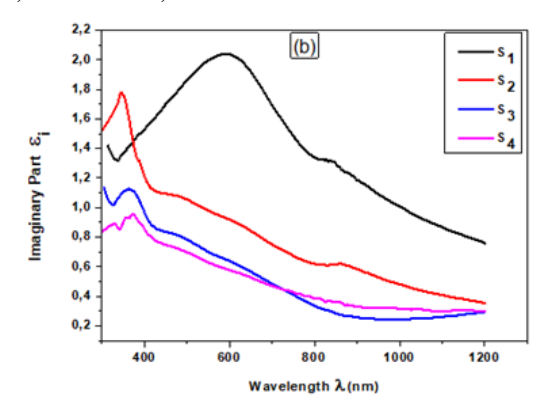
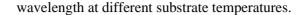
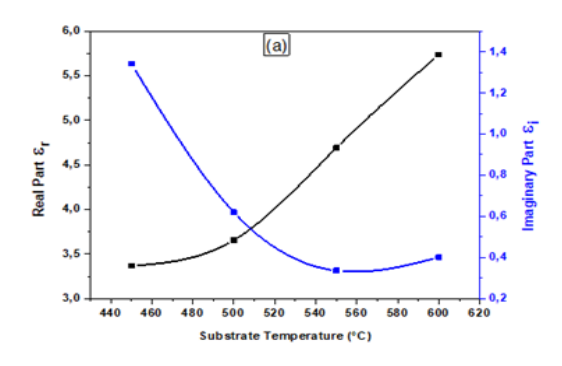


Fig. 8. Real part (a) and Imaginary part (b) of the dielectric constant as a function of

Nanotechnology Perceptions Vol. 20 No.6 (2024)





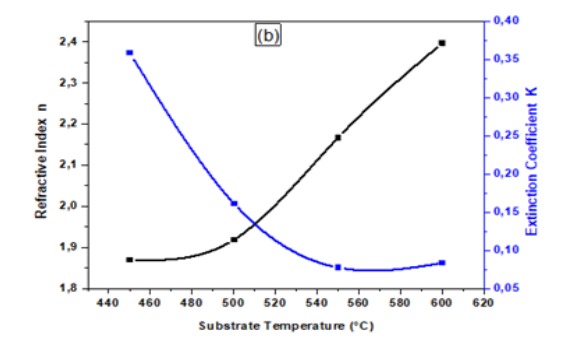


Fig. 9. Variation of dielectric constants at \square =800 nm as a function of substrate temperature: (a) ε_r and ε_i , (b) n and k.

Electrical properties:

Electrical properties are important in studying thin films designed for optoelectronic applications. The only property accessible here is the electrical conductivity (σ). To calculate it, we measure the sheet resistance (R_{sh}) using a four-points probe technique. The conductivity values of the thin films are calculated from the following formula [66]:

$$\sigma = 1/R_{sh} \times d$$
(14)

Where d is the thickness of the films.

The values of electrical conductivity of the samples are listed in Table 4, along with the electrical resistivity ($\rho = 1/\sigma$). It is noticed that the electrical resistivity decreased and increased with increasing substrate temperatures. On the other hand, we can see from Table 4 that the conductivity values increase and then decrease according to the film thickness. The electrical resistivity showed similar behavior as compared with the deposited pure CuO with a change in the substrate temperature in reference [60]. As seen in Table 4, when the resistivity has a maximum value at 550°C, the conductivity of thin films has a minimum value at the same substrate temperature. These results appeared at the film thickness 694,12 nm at a temperature of 550°C, also, this indicates that substrate temperature at this value is the optimum rate of thermal energy as mentioned above in our study. The sample S₄ showed unusual values that are not acceptable in scientific analysis and may be due to a rise in the substrate temperature which greatly affected the electrical properties. We can say all the properties of the thin films depend upon the substrate temperature, and the change in one property may have effects on the other properties, thus almost all properties are interdependent. The main effect starts from a change in the structure at depositing films. Physically the oxygen molecules are first adsorbed onto the thin film surface and the transition from physical to chemical adsorption then takes place by the capture of conduction band electrons. This phenomenon affects the mobility of the charge carrier, which leads to enhanced chemisorption of oxygen at the grain boundaries, which alters the barrier size. Since a small grain boundary area, compared to the film surface, leads to a change in the

charge carrier density and structure of the films [67]. Therefore, we observed change in the properties of the films such as crystallization, grain size, surface morphology, transmittance, dielectric constant, band gap, resistivity, and conductivity.

Table 4: The values of electrical parameters of the studied samples.

Sample	d (nm)	ρ(Ω cm)	σ (Ω cm) ⁻¹
S_1	641,79	3,5930	0,2783
S_2	721,80	3,1605	0,3164
S_3	694,12	3,7804	0,2645
S_4	735,87	-	-

4. Conclusion

We have successfully deposited a mixture of copper oxide and calcium oxide on the glass substrate. The pneumatic spray pyrolysis as economic and simple technique was used to produce the films. It is a fast and low-cost technique and requires no sophisticated specialized setup. We have prepared a series of thin films of CuO-CaO₂ for which we varied the substrate temperature from 450 to 600 °C with fixed source molarity of 0.1mol/l. It was remarked that the film prepared at 550 °C has the best crystallinity level as compared to the others, in particular for structural properties and the highest transmittance observed in the visible region. The films showed good adherence to the substrates using scratch test and no porous or hollow particles were observed. The electrical conductivity at room temperature was found in the order of 10^{-1} (Ω cm)⁻¹. The real part of the dielectric constant varied from 3.36 to 5.73 depending on the substrate temperature. Urbach's energy decreased from 0.98 to 0.85 eV with increasing substrate temperature. It was clearly observed from optical analysis that substrate temperature has a strong effect on the optical properties of the films. All optical parameters such as refractive index, extinction coefficient, band gap energy, and dielectric constants were calculated depending on the reflectance/transmittance data. In comparison, the values of the real part of the dielectric constant are higher than the values of electrical conductivity with changes in substrate temperatures. Finally, the film deposited at a substrate temperature of 550 °C has a thickness of 694,12 nm, a maximum value of transmittance, band gap 2,80 eV, and good crystallization, it may be suitable for optoelectronic devices where thin films with high transmittance and dielectric constant are required. This work can be extended to optimize the other pneumatic spray pyrolysis technique parameters such as deposition time, solution concentration, and flow rate. Thus films with good quality and better suitable optoelectronic properties can be produced.

Declaration of interest

The authors have no relevant financial or non-financial and no conflicts interests to declare.

Funding

This research did not receive any specific grant from funding agencies in the public, commercial, or not-for-profit sectors.

Author contributions:

Sayad Mostefa: Conceptualization; Data curation; Formal analysis, Investigation; Methodology; Visualization; Writing original draft, Ouahab Abdelouahab: Formal analysis *Nanotechnology Perceptions* Vol. 20 No.6 (2024)

Investigation; Methodology; Project administration; Resources; Software; Supervision; Validation; Writing - review & editing, Belakroum Karima: Co-Supervision; Formal analysis Investigation; Validation; Writing - review. Rahmane Saâd: Formal analysis Investigation; Methodology; Project administration; Resources, Kater Aicha: Data curation; Formal analysis Investigation; Methodology, Hettal Souheila: Data curation; Formal analysis Investigation; Methodology, Ben Messaoud Ouarda Data curation; Formal analysis Investigation; Methodology.

Acknowledgments

The authors would like to thank the Ministry of Higher Education and Scientific Research of Algeria for the financial support and Laboratory of Thin Films Physics and Applications (LTFPA), Mohamed Khaider Biskra University for hosting me.

References

- [1] V. Jagadeesan, V. Subramaniam, Comparison studies of Zn-doped CuO thin films deposited by manual and automated nebulizer-spray pyrolysis systems and their application in heterojunction-diode fabrication, Journal of Sol-Gel Science and Technology 102 (2022) 614–627.
- [2] M.J. Ismail, Z.T. Khodair, M.M. Kareemb, Study the structural properties of Mn-doped CuO thin films prepared by chemical spray pyrolysis technique, Materials Today: Proceedings 49 (2022) 3558-3567.
- [3] R.M. Thyab, M.A.H. Al-Hilo, F.A. Yasseen, H. Alshater, E.G. Blall, M.A. Abdel-Lateef, Influence of Aluminum Doping on Structural and Optical Properties of the Nanostructured Copper Oxide Thin Films Prepared by CSP Method, NeuroQuantology 20 (2022) 99-104.
- [4] S.S.K. Jacob, I. Kulandaisamy, S. Valanarasu, A. M.S. Arulanantham, M. Shkir, A. Kathalingam, N. Soundaram, Improving the conductivity of cuprous oxide thin films by doping Calcium via feasible nebulizer spray technique for solar cell (FTO/ZnO/Ca-Cu2O), Mater. Res. Express 6 (2019) 046405.
- [5] S.C. Ray, Preparation of copper oxide thin film by the sol-gel-like dip technique and study of their structural and optical properties, Solar Energy Materials & Solar Cells 68 (2001) 307-312.
- [6] R.D. Prabu, S. Valanarasu, V. Ganesh, M. Shkir, S. AlFaify, A. Kathalingam, S.R. Srikumar, R. Chandramohan, An effect of temperature on structural, optical, photoluminescence and electrical properties of copper oxide thin films deposited by nebulizer spray pyrolysis technique, Materials Science in Semiconductor Processing 74 (2018) 129-135.
- [7] E.M. Alkoy, P.J. Kelly, The structure and properties of copper oxide and copper aluminum oxide coatings prepared by pulsed magnetron sputtering of powder targets, Vacuum 79 (2005) 221–230.
- [8] N. Kumar, S.S. Parui, S. Limbu, D.K. Mahato, N Tiwari, R.N. Chauhan, Structural and optical properties of sol-gel derived CuO and Cu2O nanoparticles, Materials Today: Proceedings 41 (2021) 237-241.
- [9] J. Morales, L. Sanchez, F. Martin, J.R. Ramos-Barrado, M. Sanchez, Nanostructured CuO thin film electrodes prepared by spray pyrolysis: a simple method for enhancing the electrochemical performance of CuO in lithium cells, Electrochimica Acta 49 (2004) 4589–4597.
- [10] Y. Li, J. Liang, Z. Tao, J. Chen, CuO particles and plates: synthesis and gas-sensor application, Materials Research Bulletin 43 (2008) 2380-2385.
- [11] B.K.H. al-Maiyaly, I. H. Khudayer, A.J. Ibraheim, Effect ambient oxidation on structural and optical properties of copper oxide thin films, International Journal of Innovative Research in Science, Engineering and Technology 3 (2014) 8694.

- [12] S.P.P. Jones, S.M. Gaw, K.I. Doig, D. Prabhakaran, E.M.H. Wheeler, A.T. Boothroyd, J. Lloyd-Hughes, High-temperature electromagnons in the magnetically induced multiferroic cupric oxide driven by intersublattice exchange, Nature Communications 5 (2014) 3787.
- [13] T.A. Aswad, T.A. Abbas, G.G. Ali, Effect of deposition time on optical properties of CuO thin film prepared by chemical bath deposition method, Digest Journal of Nanomaterials and Biostructures 16 (2021) 831–838.
- [14] A.Tombak, M. Benhaliliba, Y.S. Ocak, T. Kiliçoglu, The novel transparent sputtered p-type CuO thin films and Ag/pCuO/n-Si Schottky diode applications, Results in Physics 5 (2015) 314–321.
- [15] A. Oral, E. Menşur, M. Aslan, E. Başaran, The preparation of copper (II) oxide thin films and the study of their microstructures and optical properties, Mater. Chem. Phys. 83 (2004) 140–144.
- [16] P. Markworth, X. Liu, J. Dai, W. Fan, T.J. Marks, R.P. Chang, Coherent island formation of Cu2O films grown by chemical vapor deposition on MgO (110), J. Mater. Res. 16 (2001) 2408–2414.
- [17] T. Mahalingam, J. Chitra, J. Chu, S. Velumani, P. Sebastian, Structural and annealing studies of potentiostatically deposited Cu2O thin films, Sol. Energy Mater. Sol. Cells 88 (2005) 209–216.
- [18] K. Santra, C. Sarkar, M. Mukherjee, B. Ghosh, Copper oxide thin films grown by plasma evaporation method, Thin Solid Films 213 (1992) 226–229.
- [19] K. Khojier, H. Savaloni, Z. Sadeghi, A comparative investigation on growth, nanostructure and electrical properties of copper oxide thin films as a function of annealing conditions, J. Theor. Appl. Phys. 8 (2014) 1–8.
- [20] A. Ogwu, T. Darma, E. Bouquerel, Electrical resistivity of copper oxide thin films prepared by reactive magnetron sputtering, J. Achiev. Mater. Manuf. Eng. 24 (2007) 172–177.
- [21] A. Ashok, G. Regmi, S. Velumani, Growth of In2Se3 Thin Films Prepared by the Pneumatic Spray Pyrolysis Method for Thin Film Solar Cells Applications, 17th International Conference on Electrical Engineering, Computing Science and Automatic Control (CCE) IEEE (2020) pp. 1-6. DOI: 10.1109/CCE50788.2020.9299133
- [22] R. Taziwa, E. Meyer, D. Katwire, L. Ntozakhe, Influence of Carbon Modification on the Morphological, Structural, and Optical Properties of Zinc Oxide Nanoparticles Synthesized by Pneumatic Spray Pyrolysis Technique, Journal of Nanomaterials 2017 (2017) 11.
- [23] R.P. Borges, P. Ferreira, A. Saraiva, R. Gonc-alves, M.A. Rosa, A.P. Gonc-alves, R.C. daSilva, S. Magalhaes, M.J.V. Lourenco, F.J.V. Santos, M. Godinho, Pulsed injection metal organic chemical vapour deposition and characterisation of thin CaO films, Physica 404 (2009) 1398–1403.
- [24] A. Yamasaki, T. Fujiwara, Electronic structure of the MO oxides (M=Mg, Ca, Ti, V) in the GW approximation, Physical Review 66 (2002) 245108.
- [25] R.C. Whited, C.J. Flaten, W.C. Walker, Exciton thermoreflectance of MgO AND CaO*, Solid State Communications 13 (1973) 1903-1905.
- [26] B.G. Nair, H. Rahman, K.A. John, K. Keerthi, S. Shaji, G.S. Okram, V. Sharma, R.R. Philip, Calcium incorporated copper indium oxide thin films a promising candidate for transparent electronic applications, Thin Solid Films 693 (2020) 137673.
- [27] G.C. Lee, Y.S. Jung, K.H. Kim, Properties of Cu2O Thin Films for All-Oxide Solar Cells, Molecular Crystals and Liquid Crystals 598 (2014) 62-68.
- [28] M.A. Alavi, A. Morsali, Ultrasonic-assisted synthesis of Ca(OH)2 and CaO nanostructures, J. Experimental Nanoscience 5 (2010) 93-105.
- [29] H. Ehrenreich, H.R. Philipp, Optical Properties of Ag and Cu, Physical Review 128 (1962) 1622.
- [30] M. Boulouz, L. Martin, A. Boulouz, A. Boyer, Effect of the dopant content on the physical properties of Y2O3–ZrO2 and CaO–ZrO2 thin films produced by evaporation and sputtering techniques, Materials Science and Engineering 67 (1999) 122–131.
- [31] G. Carta, N. El Habra, G. Rossetto, P. Zanella, M. Casarin, D. Barreca, C. Maragno, E. Tondello,

- MgO and CaO stabilized ZrO2 thin films obtained by Metal Organic Chemical Vapor Deposition, Surface & Coatings Technology 201 (2007) 9289–9293.
- [32] A. Hussain, S. Mehmood, M.N. Rasool, S. Aryal, P. Rulis, W.Y. Ching, Electronic structure, mechanical, and optical properties of CaOAl2O3 system: a first principles approach, Indian Journal of Physics 90 (2016) 917–929.
- [33] B.M. Silva, J. Oliveira, T. Rebelo, V.B. Isfahani, P. Rocha-Rodrigues, N. Lekshmi, J.H. Belo, F.L. Deepak, A.M.L. Lopes, J.P. Araújo, B.G. Almeida, Synthesis, structural and dielectric properties of Ca3Mn2O7 thin films prepared by pulsed laser deposition, Materials Research Bulletin 158 (2023) 112066.
- [34] C. Wen, M. Lanza, Calcium fluoride as high-k dielectric for 2D electronics, Applied Physics Reviews 8 (2021) 021307.
- [35] P. Bharti, B. Singh, R.K. Dey, Process optimization of biodiesel production catalyzed by CaO nanocatalyst using response surface methodology, J. Nanostructure in Chemistry 9 (2019) 269–280.
- [36] A. Bouibes, A. Zaoui, A route to possible civil engineering materials: the case of high-pressure phases of lime, Scientific Reports 5 (2015) 12330.
- [37] Z. Zeng, K. Natesan, Fabrication of CaO insulator coatings by MOCVD for application in vanadium/lithium blankets, Fusion Engineering and Design 70 (2004) 87–93.
- [38] P.N. Nirmala, G. Suresh, Influence of the particle size on the optical properties of CaO thin film, Inter. J. Recent Scientific Res. 4 (2013) 1320-1322.
- [39] I.R. Bellobono, E. Selli, L. Righetto, F. MUFFATO, Flow dynamical characterization of sorbents immobilized as composites in membranes prepared by photochemical grafting onto polymers, Mate. Chem. and Phys. 19 (1988) 131-146.
- [40] O.B. Koper, I. Lagadic, A. Volodin, K.J. Klabunde, Alkaline-Earth Oxide Nanoparticles Obtained by Aerogel Methods. Characterization and Rational for Unexpectedly High Surface hemical Reactivities, Chemistry of Materials 9 (1997) 2468-2480.
- [41] S. Kumar, V. Sharma, J.K. Pradhan, S.K. Sharma, P. Singh, J.K. Sharma, Structural, Optical and Antibacterial Response of CaO Nanoparticles Synthesized via Direct Precipitation Technique, Nano Biomed. Eng. 13 (2021) 172-178.
- [42] Z. Yu, J. Xue, Q. Yao, G. Hui, Y. Jiang, W. Xue, Annealing-free copper source-drain electrodes based on copper–calcium diffusion barrier for amorphous silicon thin film transistor, Thin Solid Films 624 (2017) 106-110.
- [43] H. Souheila, O. Abdelouahab, R. Saâd, B. Ouarda, K. Aicha, S. Mostefa, Effect of the Number of Dips on the Properties of Copper Oxide Thin Films Deposited by Sol-Gel Dip-Coating Technique, I. J. of Materials Science and Engineering 19 (2022) 1-8.
- [44] A. Hafida, R. Saâd, H. Souheila, K. Nabila, Precursor nature and molarities effect on the optical, structural, morphological, and electrical properties of TiO2 thin films deposited by spray pyrolysis, Optik 203 (2020) 163985.
- [45] K. Nabila, R. Saâd, A. Abdelkrim, Substrate temperature-dependent properties of sprayed cobalt oxide thin films, J Mater Sci: Mater Electron. 30 (2018) 1153–1160.
- [46] M. Manickam, V. Ponnuswamy, C. Sankar, R. Suresh, Cobalt Oxide thin films prepared by NSP Technique: Impact of molar concentration on the Structural, Optical, Morphological and Electrical properties, Optik 127 (2016) 5278–5284.
- [47] A. Ilya Ovid'ko, Interfaces and misfit defects in nanostructured and polycrystalline films, Rev. Adv. Mater. Sci. 1 (2000) 61-107.
- [48] N. Kouidri, S. Rahmane, Effect of cobalt chloride concentration on structural, optical and electrical properties of Co3O4 thin films deposited by pneumatic spray, J. New Technol. Mater. 10 (2020) 56-62.
- [49] S. Kose, F. Atay, V. Bilgin, I. Akyuz, Some physical properties of copper oxide films: The effect of substrate temperature, Materials Chemistry and Physics 111 (2008) 351–358.

- [50] Y. Bellal, A. Bouhank, H. Serrar, T. Tüken, G. Sığırcık, A Copper Oxide (CuO) Thin Films Deposited by Spray Pyrolysis Method, MATEC Web of Conferences 253 (2019) 03002. https://doi.org/10.1051/matecconf/201925303002
- [51] N. Ghrairi, M. Bouaicha, Structural, morphological, and optical properties of TiO2 thin films synthesized by the electrophoretic deposition technique, Nanoscale Research Letters 7 (2012) 357.
- [52] M. Fang, H. He, B. Lu, W. Zhang, B. Zhao, Z. Ye, J. Huang, Optical properties of p-type CuAlO2 thin film grown by rf magnetron sputtering, Applied Surface Science 257 (2011) 8330–8333.
- [53] V. JANAKIRAMAN, V. TAMILNAYAGAM, R.S. SUNDARARAJAN, S. SIVABALAN, B. SATHYASEELAN, Physiochemical properties of tin oxide thin films deposited by spray pyrolysis, Digest J. Nanomater. Biostruct. 15(3) (2020) 849 855.
- [54] S.H. Salman, A.A. Shihab, A-H.Kh. Elttayef, Studying The Effect of The Type of Substrate on The Structural, Morphology and Optical Properties of TiO2 Thin Films Prepared by RF Magnetron Sputtering, Energy Procedia 157 (2019) 199–207.
- [55] C. Bouzidi, H. Bouzouita, A. Timoumi, B. Rezig, Fabrication and characterization of CuAlO2 transparent thin films prepared by spray technique, Materials Science and Engineering 118 (2005) 259–263.
- [56] A. Mannu, M.E.D. Pietro, A. Mele, Band-Gap Energies of Choline Chloride and Triphenylmethylphosphonium bromide-Based Systems, Molecules 25(7) (2020) 1495.
- [57] Sh.J. Ikhmayies, R.N. A-Bitar, A study of the optical bandgap energy and Urbach tail of spray-deposited CdS:In thin films, j. mater. Res. technol. 2 (2013) 221–227.
- [58] O. Diachenko, J.Jr. Kováč, O. Dobrozhan, P. Novák, J. Kováč, J. Skriniarova, A. Opanasyuk, Structural and Optical Properties of CuO Thin Films Synthesized Using Spray Pyrolysis Method, Coatings 11 (2021) 1392.
- [59] P. DATTA, M. SHARMIN, J. PODDER, S. CHOUDHURY, Influence of substrate temperature on the morphological, structural, optical and electrical properties of nanostructured CuO thin films synthesized by spray pyrolysis technique, J. Optoelectronics and Advanced Materials 23(1-2) (2021) 35-42.
- [60] S. Cho, Optical and Electrical Properties of CuO Thin Films Deposited at Several Growth Temperatures by Reactive RF Magnetron Sputtering, Met. Mater. Int. 19(6) (2013) 1327-1331.
- [61] M.DI. GIULIO, G. MICOCCI, R. RELLA, P. SICILIANO, A. TEPORE, Optical absorption and photoconductivity in amorphous indium selenide thin films, Thin Solid Films 148 (1987) 273-278.
- [62] A. Paliwal, A. Sharma, M. Tomar, V. Gupta, Optical properties of WO3 thin films using surface plasmon resonance technique, J. Applied Physics 115 (2014) 043104.
- [63] A. Moumen, B. Hartiti, Ph. Thevenin, M. Siadat, Synthesis and characterization of CuO thin films grown by chemical spray pyrolysis, Optical and Quantum Electronics 49 (2017) 70.
- [64] K.R. Rajesh, C.S. Menon, Estimation of the refractive index and dielectric constants of magnesium phthalocyanine thin films from its optical studies, Materials Letters 53 (2002) 329–332.
- [65] E.A. El-Wahabb, A.E. Bekheet, Effect of annealing on the optical properties of Ag33Sb31Se36 thin films, Applied Surface Science 173 (2001) 103–114.
- [66] A. Abdelkrim, R. Saâd, K. Nabila, A. Hafida, O. Abdelouahab, Polycrystalline SnO2 thin films grown at different substrate temperature by pneumatic spray, J Mater Sci: Mater Electron. 28 (2017) 4772–4779.
- [67] R.R. Kasar, N.G. Deshpande, Y.G. Gudage, J.C. Vyas, R. Sharma, Studies and correlation among the structural, optical and electrical parameters of spray-deposited tin oxide (SnO2) thin films with different substrate temperatures, Physica 403 (2008) 3724–3729.